Lungs of patients with acute respiratory distress syndrome show diffuse inflammation in normally aerated regions: A [18F]-fluoro-2-deoxy-D-glucose PET/CT study

Giacomo Bellani, MD; Cristina Messa, MD; Luca Guerra, MD; Ester Spagnolli, MD; Giuseppe Foti, MD; Nicolò Patroniti, MD; Roberto Fumagalli, MD; Guido Musch, MD; Ferruccio Fazio, MD; Antonio Pesenti, MD

Objective: **Neutrophilic inflammation plays a key role in the pathogenesis of acute respiratory distress syndrome (ARDS) and acute lung injury (ALI). Positron emission tomography (PET) with [^{18}F]-fluoro-2-deoxy-D-glucose (^{18}FDG) can be used to image cellular metabolism that, during lung inflammatory processes, likely reflects neutrophils activity. The aim of this study was to assess the magnitude and regional distribution of inflammatory metabolic activity in the lungs of patients with ALI/ARDS by PET with ^{18}FDG.**

Design: **Prospective clinical investigation.**

Patients: **Ten patients with ALI/ARDS; four spontaneously breathing and two mechanically ventilated subjects, without known lung disease, served as controls.**

Interventions: **In each individual we performed an ^{18}FDG PET/computed tomography of the thorax.**

Measurements and Main Results: **^{18}FDG cellular influx rate constant (K_i) was computed for the imaged lung field and for regions of interest, grouping voxels with similar density. In all patients with ALI/ARDS, K_i was higher than in controls, also after accounting for the increased lung density. K_i values differed greatly among patients, but in all patients K_i of the normally aerated regions was much higher (2- to 24-fold) than in controls. Whereas in some patients the highest K_i values corresponded to regions with the lowest aeration, in others these regions had lower K_i than normally and mildly hypoaerated regions.**

Conclusion: **In patients with ALI/ARDS, undergoing mechanical ventilation since days, the metabolic activity of the lungs is markedly increased across the entire lung density spectrum. The intensity of this activation and its regional distribution, however, vary widely within and between patients. (Crit Care Med 2009; 37:2216–2222)**

KEY WORDS: artificial respiration; adult respiratory distress syndrome; positron-emission tomography; mechanical ventilators; x-ray computed tomography

Acute lung injury (ALI) and acute respiratory distress syndrome (ARDS) are associated with a high mortality and significant long-term morbidity (1–3). Although ALI/ARDS was originally considered to affect the lung diffusely, computed tomography (CT) studies indicated that the areas of lung with normal aeration could be preserved, and coexist with poorly and nonaerated tissue, leading to the "baby-lung" concept (4).

It is accepted that the inflammation and neutrophils (PMNs) play a key role in ALI/ARDS (5–7) and that their accumulation is a hallmark of ALI, despite the fact that ARDS can develop in severely neutropenic patients (8). Furthermore, PMNs are primary effectors of ventilator-induced lung injury (9–11), which can aggravate ALI/ARDS.

Positron emission tomography (PET) with [^{18}F]-fluoro-2-deoxy-D-glucose (^{18}FDG) (12–16) can be used to image and quantitate cellular metabolic activity *in vivo*. In several lung inflammatory processes, both in humans (17, 18) and in animal models (19–23), the increased metabolic activity can be ascribed, almost exclusively, to PMNs activation.

In patients with ALI/ARDS, it is unknown whether PMNs activation is diffused throughout the entire lung, similarly to what has been suggested for the increase in vascular permeability (24), or if it is patchy, as is the increase in lung density (25). Gaining knowledge on the distribution of PMNs activity and its relationship to lung density is important, because it could offer insights into the pathophysiology of ALI/ARDS. For example, metabolic activation confined to poorly and nonaerated areas would indicate that the baby lung is spared by activated inflammatory cells, whereas activation confined to aerated areas would suggest that regional collapse may protect tissue from inflammatory cells activation, triggered instead by ventilatory stretch. Furthermore, knowing the intensity and/or the regional distribution of the inflammatory process might lead to better tailoring of individual therapeutic and ventilatory strategies. However, the methods currently available to monitor the presence of PMNs in the lungs, like bronchoalveolar lavage (26) and lung biopsy (27), are unable to provide comprehensive information on the topographical distribution of lung involvement.

Consequently, we combined ^{18}FDG-PET and CT imaging to assess the magnitude and

From the Department of Experimental Medicine (GB, ES, AP, RF), 'Centro Bioimmagini Molecolari' (CM, FF), University of Milan-Bicocca, Monza (MI), Italy; Department of Perioperative Medicine and Intensive Care (GB, ES, AP, RF, GF, NP), Nuclear Medicine Unit (LG), San Gerardo Hospital, Monza (MI), Italy; Institute of Molecular Bioimaging and Physiology (CM, FF), National Research Council, Milano, Italy; Department of Anesthesia and Critical Care (GM), Massachusetts General Hospital, Harvard Medical School, Boston, MA.

Supported, in part, by a grant from the European Society of Intensive Care Medicine (ECCRN Young Investigator Award 2006) and by a national grant of the Italian Ministry of Education, University and Research (FIRB 2001 and Fondo di Internazionalizzazione 2005).

This work was performed at the University of Milan-Bicocca and San Gerardo Hospital, Monza, Italy.

The authors have not disclosed any potential conflicts of interest.

For information regarding this article, E-mail: antonio.pesenti@unimib.it

DOI: 10.1097/CCM.0b013e3181aab31f

spatial distribution of PMNs activity and test whether activation occurred only within a certain lung density range.

MATERIALS AND METHODS

Investigational Protocol. The protocol was approved by our institution's ethical committee and informed consent was obtained according to the committee's recommendations. Patients were recruited from the general intensive care unit (ICU) of a university hospital.

Inclusion criteria were as follows:

- Diagnosis of ALI/ARDS according to the 1994 European/American Consensus conference (28), requiring mechanical ventilation.
- Planning by the attending physician of a thorax CT scan as a part of the patient's clinical management.

Exclusion criteria were as follows:

- Pregnancy
- Age <18 years
- Impossibility of patient's transport according to the attending physician
- Lung surgery in the last 4 weeks
- Oliguria (urinary output $<0.5\ mL \cdot kg^{-1} \cdot hr^{-1}$) or anuria
- Known or suspected cancer
- History of chronic lung disease
- Logistic reasons (e.g., PET/CT camera unavailable until patient had lost eligibility criteria).

Once a patient was judged eligible for the study, the PET/CT scan was scheduled, usually within 1 or 2 days; on the day of the study, eligibility was confirmed. Ten patients were enrolled from September 2006 to October 2007. The PET/CT study being usually performed around 2 PM, the enteral or parenteral nutrition and any glucose-containing infusion were stopped at 6 AM to ensure a fasting period of at least 6–8 hours. In patients undergoing insulin therapy, this was stopped as well. Before transport from the ICU to the PET/CT facility, blood glucose was tested to confirm a level between 80 and 140 mg/dL.

Before transport, the following variables were measured with the patient on volume-controlled ventilation at settings selected by the attending physician: hemodynamic variables (heart rate, invasive arterial blood pressure, central venous pressure and, if a pulmonary artery catheter was in place, pulmonary arterial pressure, pulmonary artery occlusion pressure, and cardiac output by thermodilution); ventilatory settings (positive end-expiratory pressure [PEEP], respiratory rate, tidal volume [V_T], mean airway pressure, F_{IO_2}). Expiratory and inspiratory pauses were performed to measure, respectively, total PEEP ($PEEP_{tot}$, which includes intrinsic PEEP) and plateau pressure (P_{plat}). Respiratory system compliance (C_{rs}) was computed as: $C_{rs} = V_T/(P_{plat} - PEEP_{tot})$.

Blood gases were measured from arterial and, if available, mixed venous samples (AVL Omni 6, Roche, Basel, Switzerland). Venous admixture was computed according to the Berggren equation (29).

During transport, and throughout the permanence in the PET/CT facility, clinical care was provided by a physician and a nurse uninvolved in the study procedures. Mechanical ventilation was provided by an ICU ventilator, and invasive arterial blood pressure, electrocardiogram, peripheral oxygen saturation and expired CO_2 were continuously monitored. Ventilatory settings, sedation, and fluid therapy were maintained constant throughout the study period, unless clinically advised.

At the end of the study, collection of the aforementioned variables was repeated in the ICU.

Finally, we recorded ICU outcome (survival or death) of each patient.

Image Acquisition and Analysis. We used a GE Discovery ST (GE Medical Systems, Milwaukee, WI) PET/CT, with an axial field of view of approximately 18 cm (47 3.27-mm-thick sections, separated by 0.48-mm intervals), equipped with an eight-slice CT. The section of thorax to be imaged was selected on the scout view just above the diaphragm. Once the selection was made, care was taken to avoid any further movement of the patient on the examination table. A spiral CT scan (140 kV, 80 mA, slice thickness 3.75 mm, no interval between slices) of the chosen section was obtained while holding the patient apneic (by switching the ventilator to constant positive airway pressure modality) at the same mean airway pressure as during mechanical ventilation, to ensure the best possible cross-registration between the CT scan and the PET acquisition to follow, performed during tidal ventilation. The patient was then advanced to the PET detector; the tomograph ensures the cross-registration of the same axial field-of-view between the CT and the PET acquisition. A bolus of ^{18}FDG (~300 MBq) was rapidly injected intravenously, 5 seconds after that the acquisition of sequential PET frames was started with the following protocol: 12 frames lasting 10 seconds each ($12 \times 10''$), $10 \times 30''$, $8 \times 300''$, $1 \times 600''$, for a total imaging time of 57 minutes.

Dynamic PET data were reconstructed by ordered-subset expectation maximization iterative algorithm (30–32) and corrected for decay, scatter, random counts, and attenuation (using CT).

Images were analyzed with a software specifically developed in the Matlab environment (Matlab R2007a, The Mathworks, Natick, MA). Lung fields (region-of-interest [ROI_L]) were manually outlined on the CT images, carefully avoiding the large airways, vessels, and pleural effusions. The ROI_L, displayed as thick yellow lines, was overlapped with the last frame of the corresponding PET scan, and the fused PET/CT image was used for a visual assessment of the location of ^{18}FDG uptake.

For quantitative image analysis, we used the graphical method of Patlak et al (33). Briefly, an additional ROI was defined in the center of the descending aorta over at least 15–20 slices (34) to determine the time course of blood activity. The activity in ROI_L divided by blood activity was plotted as a function of the integral of blood activity divided by blood activity (Fig. 1). After a steady state in cellular

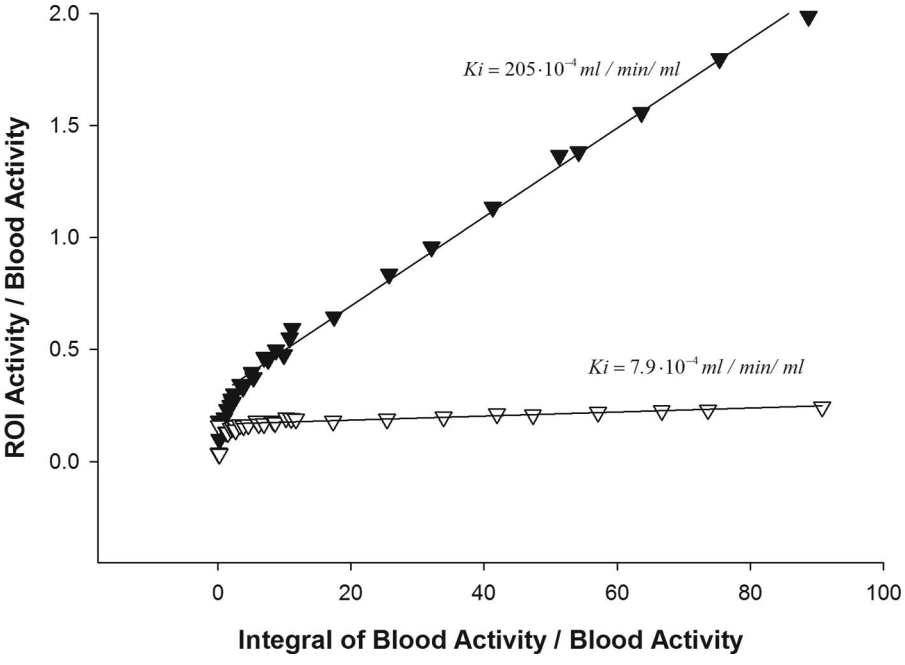

Figure 1. Representative Patlak plot for a patient with acute respiratory distress syndrome (corresponding in the tables to patient 4, *filled symbols*) and for a spontaneously breathing control subject (*empty symbols*). [^{18}F]-fluoro-2-deoxy-D-glucose activity in a region of interest (*ROI*), divided by blood activity, is plotted as a function of the time integral of blood activity divided by blood activity. The slope of the linear part of this relationship corresponds to the uptake rate of [^{18}F]-fluoro-2-deoxy-D-glucose (K_i).

^{18}FDG uptake is reached, the plot follows a straight line, for which the slope indicates the ^{18}FDG uptake rate constant (K_i). Because this parameter is expected to increase with the number of cells per voxel (e.g., in the case of increased CT density due to an increase in the ratio of pulmonary parenchyma-to-gas volume), we also normalized K_i by the mean fractional density of the lung, computed as $(CT_{MEAN} + 1000)/1000$, where CT_{MEAN} is the average CT number of the ROI_L: $K_{iDENS} = K_i/([CT_{MEAN} + 1000]/1000)$.

The original CT matrix, with a size of 512×512 pixels, was rescaled to achieve the same dimension (128×128) and pixel size (4.5 mm) of the original PET image. This scaling process lowers the spatial resolution of CT to a level similar to that of PET. To describe the intra-patient relationship between lung density and ^{18}FDG uptake, the original ROI_L was subsegmented (relying on the downscaled CT image) by allocating all the voxels within "bins" that were 100 Hounsfield Units (HU) wide (the first "submask" enclosed all the voxels between −1000 HU and −900 HU, the second one comprised all the voxels between −900 HU and −800 HU, and so forth). For each of these density-defined ROIs the K_i (K_{iD}) and mean CT values (CT_D) were computed. We emphasize that K_{iD}, as opposed to K_{iDENS}, is not a density-normalized K_i, rather it is a measure of the ^{18}FDG uptake rate of lung areas with a given density. Finally, using the same binning procedure, we defined normally aerated ROIs (comprising voxels with CT attenuation between −900 and −501 HU) and "collapsed or consolidated" (i.e., nonaerated) ROIs (comprising voxels with CT attenuation between −100 and +100 HU), and we computed their K_i (K_{iNA} and K_{iCO}, respectively). None of the aforementioned calculations was performed on a voxel-by-voxel basis, rather on the activity arising from a given ROI, which is the average activity of the voxels in the ROI.

We also computed the relative weight of the normally aerated and nonaerated (−100 HU < CT < 100 HU) tissue, by summing the weight of the corresponding voxels and dividing it by the weight of the entire ROI_L. The weight of each voxel was computed as $([CT_{vox} + 1000]/1000) \times Vol_{vox}$, where CT_{vox} and Vol_{vox} are the CT number and the volume of the voxel, respectively.

Control Data. To obtain control values, the same imaging protocol and data analysis were performed:

a. In four spontaneously breathing subjects, undergoing PET/CT for clinical indications, without a known pulmonary disease;
b. In two ICU patients, being mechanically ventilated (for 4 and 19 days) for a neurologic disorder, who had normal gas exchange (Pao_2/Fio_2 >300 mm Hg).

Statistics. SPSS 14.0 was used for statistical analysis (SPSS, Chicago, IL). Although variables were normally distributed (as assessed by Kolgomorov-Smirnov *Z* test), given the relatively small sample size and the difference in size among groups, we chose to use the nonparametric Mann-Whitney *U* test for comparison among groups. Wilcoxon's signed-rank test was used for paired comparisons (baseline vs. after PET/CT). Linear regression was used to assess correlation among variables. A p value <0.05 was considered statistically significant.

RESULTS

The main demographic and clinical characteristics of the patients are shown in Table 1. None of these parameters differed between before and after the PET/CT study (data not shown).

In patients with ALI/ARDS, the metabolic activity of the lungs was markedly elevated in comparison with controls, as shown by the K_i values (Fig. 2). This difference persisted after normalizing K_i by lung density (K_{iDENS}).

The intersubject variability of K_i and K_{iDENS} was large (coefficients of variation were 67.8% and 59.8%, respectively). K_i did not correlate with mean lung density (CT_{mean}, $r^2 = .15$) or with the relative weight of either nonaerated ($r^2 = .21$) or normally aerated tissue ($r^2 = .14$). However, K_i correlated negatively with Pao_2/Fio_2 (Fig. 3; $r^2 = .48$, $p < 0.05$). Although attempting to assess the relationship between lung metabolic activity and the po-

Table 1. Main demographic, clinical, and physiologic patient characteristics

	Patient No.										
	1	2	3	4	5	6	7	8	9	10	Mean ± SD
Age, yrs	75	71	71	62	47	62	70	73	74	59	66.4 ± 8.8
Sex, M:F	F	M	F	M	M	M	M	M	M	M	8:2
ARDS etiology, Pulm:ExP	Cryoglobulinemia (ExP)	Ab Ingestis (Pulm)	Sepsis (ExP)	Mefloquine-induced pneumonitis (Pulm)	Sepsis (ExP)	Hemorrhagic alveolitis (Pulm)	Sepsis (ExP)	HAP (Pulm)	CAP (Pulm)	CAP (Pulm)	6:4
Outcome at ICU discharge, S:D	D	S	S	D	D	D	S	S	S	S	6:4
Time on MV before study, days	2	0	7	6	14	3	10	2	3	7	5.4 ± 4.3
Heart rate, bpm	53	92	105	79	86	92	77	65	83	73	80.5 ± 14.8
MAP, mm Hg	88	81	70	83	78	102	74	84	100	57	81.7 ± 13.4
MPAP, mm Hg	30	30	N/A	24	31	39	N/A	24	28	28	29.2 ± 4.7
Pao_2/Fio_2, mm Hg	185	197	149	93	157	138	194	180	217	120	163 ± 39
$Paco_2$, mm Hg	34	42	33	57	46	41	39	45	53	61	45.1 ± 9.4
Fio_2	0.50	0.65	0.60	0.80	0.50	0.50	0.55	0.60	0.40	0.85	0.59 ± 0.14
Venous admixture	0.28	0.26	N/A	0.37	0.30	0.31	N/A	0.23	0.24	0.28	0.28 ± 0.04
$PEEP_{tot}$, cm H_2O	13	12	9	13	14	16	12	10	10	15	12.4 ± 2.3
Tidal volume, mL/kg	6.8	6.0	10.0	6.3	7	6.6	6.8	7.0	6.4	5.4	6.8 ± 1.2
Plateau pressure, cm H_2O	33	23	18	27	28	25	25	18	17	31	24.6 ± 5.7
Respiratory rate, bpm	30	24	20	20	30	24	28	16	20	32	24.4 ± 5.4
Minute ventilation, L/min	11	12.1	10.1	11.1	12.1	10.9	10.8	7.3	8.8	11.7	10.6 ± 1.5
Blood glucose, mg/dL	125	136	118	138	111	137	127	102	130	96	122 ± 15

M, male; F, female; HAP, hospital acquired pneumonia; CAP, community acquired pneumonia; ICU, intensive care unit; S, survived; D, deceased; Pulm, pulmonary; ExP, extrapulmonary; MV, mechanical ventilation; $PEEP_{tot}$, total positive end-expiratory pressure (including intrinsic-PEEP); MAP, mean arterial pressure; MPAP, mean pulmonary arterial pressure; N/A, not available.

In patients without a Swan-Ganz catheter, venous admixture and MPAP are not available. Each patient's characteristics given on the day of the study, collected before transport to the positron emission tomography/computed tomography facility. For dichotomic variables, the last column reports the ratio between the two groups.

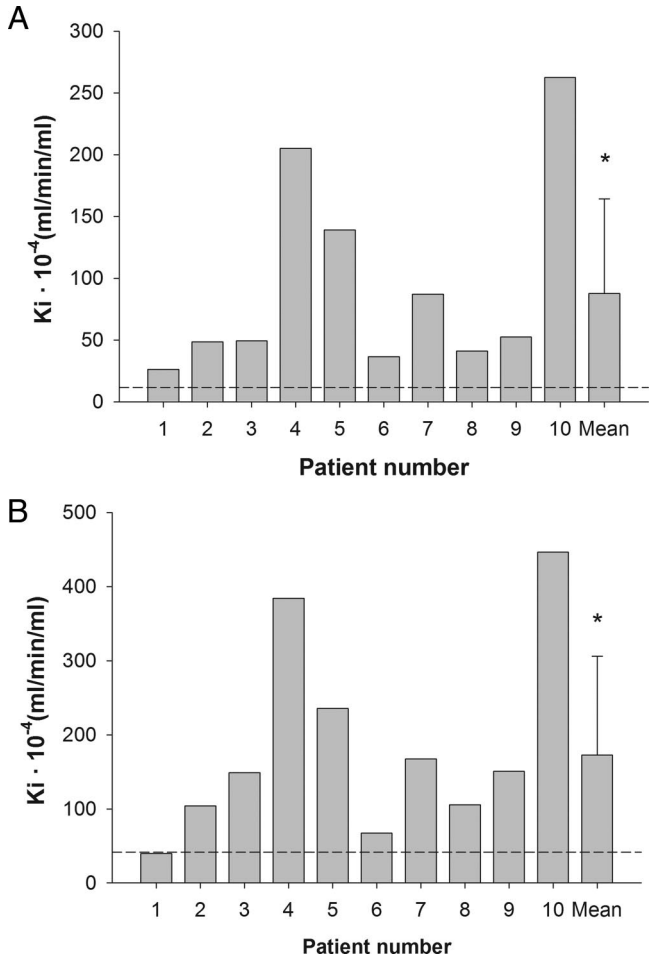

Figure 2. [^{18}F]-fluoro-2-deoxy-D-glucose uptake rate (K_i) of the imaged lung (*A*), in the individual patients and as mean ± SD. Despite large between-patients variability, K_i was higher than that of control subjects (dashed line denotes mean K_i of controls). This could not be ascribed solely to increased lung density, because the difference persisted after normalization by lung density (*B*). *$p <$ 0.05 patients vs. controls.

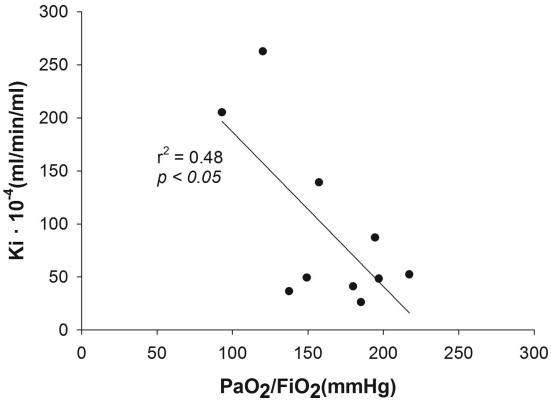

Figure 3. Correlation among the metabolic activities of lungs, expressed as uptake rate of [^{18}F]-fluoro-2-deoxy-D-glucose (K_i), and Pao_2/Fio_2.

tential injury arising from mechanical ventilation, we could not find significant correlations between either K_i or K_{iDENS} and P_{plat} or duration of mechanical ventilation, although when assessed by Spearman's correlation coefficient both K_i and K_{iDENS} were correlated with duration of mechanical ventilation ($p < 0.05$ for both).

The metabolic activity of the normally aerated tissue (K_{iNA}) of patients with ALI/ARDS showed, on average, greater than seven-fold increase compared with controls (Table 2). In the two patients undergoing mechanical ventilation without ALI/ARDS, K_{iNA} was 16.5 and 7.1×10^{-4} mL·min^{-1}·mL^{-1}.

When qualitatively describing the regional distribution of ^{18}FDG uptake, we recognized different patterns among patients. While in five patients (50%) ^{18}FDG uptake was highest in regions with the highest density and progressively decreased in regions with lower density (Fig. 4*A*), in three patients (30%) regions with normal or mildly decreased aeration had ^{18}FDG uptake similar to or greater than that of regions with lower aeration (Fig. 4*B*). Finally, in two patients, ^{18}FDG uptake was lower than in the other patients and homogenously distributed throughout the lungs.

Analogous results were found when plotting the K_{iD} values as a function of the respective CT_D values (Fig. 5). In three patients, the shape of the relationship between CT_D and K_{iD} was very different from the rest of the population, as the highest K_{iD} values occurred in the density range of normally or poorly aerated voxels rather than in nonaerated voxels.

DISCUSSION

This study shows that the lungs of patients with ALI/ARDS have an intense metabolic activity, likely to arise from activated PMNs. The magnitude and distribution of this activity were variable among patients. However, a consistent finding was that metabolic activation did not involve only nonaerated areas of the lung with severe loss of aeration, but also areas detected by CT as being "normally aerated" (the "baby lung"). Furthermore, although the increase in regional metabolic activity paralleled that in density in some patients, other patients showed higher metabolic rate in areas with normal or mildly reduced aeration than in areas with severe loss of aeration.

We enrolled a small and heterogeneous cohort of patients, mainly because of the clinical and logistic difficulties of a study like this. For the same reasons, we could not study all patients at the same time point in the course of illness. However, while the small number of patients can be seen as a limitation, and may make some of our inferences somewhat speculative, we believe that the heterogeneous sample enrolled is representative of the patient population with ALI/ARDS treated at our institution.

Table 2. Image-derived parameters

	Patients with ALI/ARDS											
	1	2	3	4	5	6	7	8	9	10	Mean ± SD	Controls, Mean ± SD
$K_{iNA} \times 10^4$ (mL·min^{-1}·mL^{-1})	23.5	30.6	37.4	198.7	145.1	31.7	42.3	31.8	37.2	260.3	83.8 ± 85.6[a]	10.9 ± 3.1
$K_{iCO} \times 10^4$ (mL·min^{-1}·mL^{-1})	26.6	101.0	128.3	172.5	109.6	48.8	151.8	76.5	134.0	263.6	121.3 ± 67.3	—
CT_{MEAN} (HU)	−343	−534	−668	−466	−409	−458	−479	−610	−652	−412	−503.2 ± 109.7[a]	−727.6 ± 62.9

ALI, acute lung injury; ARDS, acute respiratory distress syndrome; K_{iNA}, K_i values (net uptake rate of ^{18}FDG, computed according to Patlak's graphical analysis [33]) of lung regions with density in the range of normal aeration (i.e., with CT attenuation between −900 and −501 HU); K_{iCO}, K_i values of lung regions with density in the range of collapse or consolidation (i.e., with CT attenuation between −100 and +100 HU); CT_{mean}, mean computed tomography value of the lungs; HU, Hounsfield units.

[a] $p < 0.05$ vs. controls. Image-derived parameters for patients with ALI/ARDS and control subjects. K_i values of controls are similar to those reported in the literature (17).

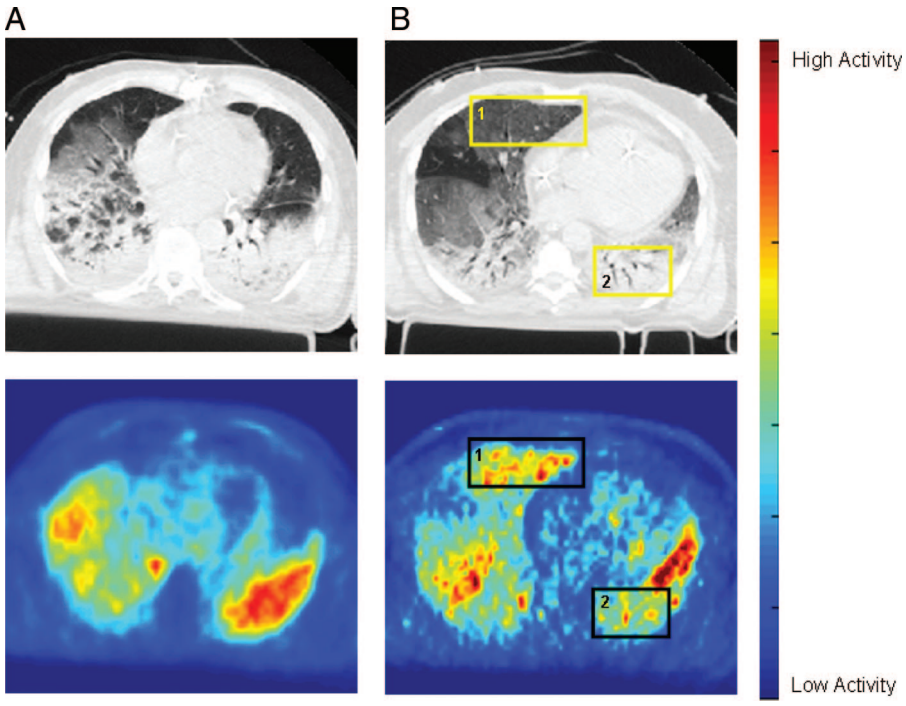

Figure 4. Representative images of cross-registered computed tomography (CT) and [^{18}F]-fluoro-2-deoxy-D-glucose (^{18}FDG) positron emission tomography from two patients with acute lung injury/acute respiratory distress syndrome. The CT image was acquired during a respiratory pause at mean airway pressure. The gray scale is centered at −500 Hounsfield Units with a width of 1250 Hounsfield Units. Positron emission tomographic images represent the average pulmonary ^{18}FDG concentration during the last 20 minutes of acquisition (from 37 to 57 minutes since ^{18}FDG administration); the color scale represents radioactivity concentration (kBq/mL). *A*, ^{18}FDG distribution parallels that of the opacities detected on CT (patient 7 in Tables). *B*, Intense ^{18}FDG uptake can be observed in normally aerated regions (patient 4 in Tables) (*square 1*), while activity is lower in the dorsal, "nonaerated" regions of both lungs (*square 2*; patient 4 in Tables).

To detect and quantify inflammation, we used PET/CT with ^{18}FDG, a technique with several advantages: low invasiveness, possibility of sampling a large fraction of the lungs, and cross registration with CT. For quantitative measurement of ^{18}FDG uptake, we computed K_i; i.e., the "influx rate constant" of the tracer. K_i expresses the net uptake of ^{18}FDG by cells (taking into account the rates of transmembrane transport and phosphorylation) and is proportional to their glycolytic activity (22). An increase in K_i could be due to increased metabolic activity of the cells or to an increased number of cells. Several points related to interpretation of the ^{18}FDG signal need to be addressed. First, ^{18}FDG is a nonspecific tracer, because it labels any cell with an intense glucose uptake. Several studies, performed both in humans (17, 18) and animal models (19, 20, 22, 23) have shown that, during pulmonary inflammatory processes, the ^{18}FDG uptake as measured by K_i can be attributed almost exclusively to activated PMNs, possibly because of the heavy dependence of these cells on anaerobic glycolysis (35). Even when macrophages are more abundant than PMNs, PMNs are the cells uptaking ^{18}FDG (19). In a model of ventilator-induced lung injury, K_i correlated with the number of PMNs detected in the lung and decreased substantially with progressive PMNs depletion (20). Furthermore, we excluded all patients with diagnosis or suspicion of cancer. For these reasons, it seems reasonable to assume that, in our patients, most of the ^{18}FDG signal arose from PMNs activated during inflammation.

Second, in patients with ALI/ARDS, as well as in normal subjects, the distribution of perfusion in the lung is not homogeneous (36, 37); however, this is unlikely to affect ^{18}FDG distribution, for which uptake has been repeatedly shown to be almost totally unrelated to regional perfusion (38–42). Indeed, in experimental models of unilateral lung injury (15, 20), the injured lung always showed greater K_i than the control lung independent of whether blood flow favored the injured lung or not.

Third, as long as the subject is normoglycemic, there does not seem to be a systematic effect of blood glucose on ^{18}FDG uptake. Indeed, in our patients, we did not find a significant correlation between blood glucose level and K_i ($r^2 = .13$, p = not significant). In this setting, normalization of ^{18}FDG uptake by blood glucose would be more likely to introduce an additional error than to improve the data quality (43, 44) and is usually not performed. Taken together, these considerations suggest that interindividual differences in blood glucose levels had no impact on K_i.

K_i values differed greatly among patients. The increase and the interindividual variability of K_i persisted when K_i was normalized by lung density, to account for the

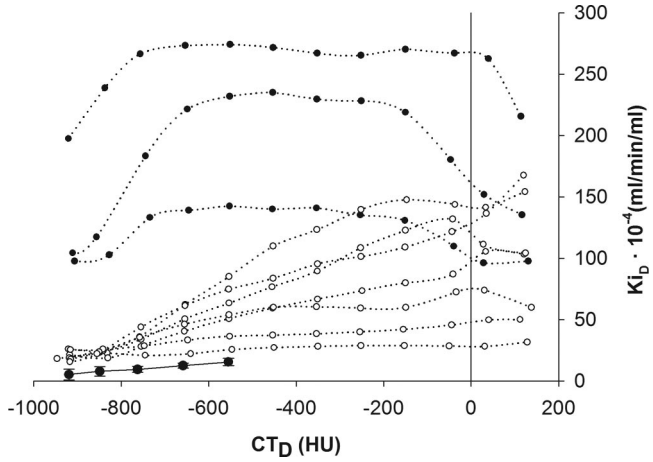

Figure 5. Distribution of regional metabolic activity (K_{iD} is the [^{18}F]-fluoro-2-deoxy-D-glucose uptake rate of areas of specified density) as a function of regional lung density (CT_D), in the patients with acute respiratory distress syndrome/acute lung injury (*dotted lines*) compared with that of the four controls (*solid line*: mean; *bars*: SD). In some patients K_{iD} increased linearly with CT_D (*empty symbols*), but this was not the case for other patients (*filled symbols*). Note that, in all patients, the metabolic rate was systematically increased across the entire spectrum of normal lung attenuation. *HU*, Hounsfield Units.

effect that a greater amount of lung tissue per unit volume of lung is expected to have on K_i. When the increase in density is due to edema, this normalization should be conservative (20), since it is expected to lead to an underestimation of metabolic rate because edema does not contribute significantly to ^{18}FDG uptake as measured by K_i (22).

In all patients with ALI/ARDS, metabolic activity was markedly increased in lung with density between −900 and −500 HU. Previous studies showed that, despite preserved aeration, the "baby lung" bears functional abnormalities. Although in the course of lobar pneumonia, endothelial permeability increased only in the affected lobe, in patients with ALI/ARDS permeability increased diffusely throughout the lung (24, 45). Our study provides direct evidence that, in patients with ALI/ARDS, the normally aerated parenchyma shows a substantially increased metabolic rate, likely to reflect the presence of activated inflammatory cells. This supports the concept that the "baby lung" is as involved by the inflammatory process as the rest of the lung, even though it maintains normal aeration. Mechanical ventilation is known as a powerful inflammatory stimulus (20, 46–49). In our population, there was a trend showing that K_i were higher in patients ventilated for a longer period; this might suggest that part of the increase in metabolic activity was due to mechanical ventilation. In the mechanically ventilated patients without ALI/ARDS, the uptake of ^{18}FDG in normally aerated tissue was similar to that of spontaneously breathing controls and significantly lower than that of patients with ALI/ARDS. This finding suggests that the increased metabolic activity in normally aerated areas of patients with ALI/ARDS is more likely due to the syndrome rather than to mechanical ventilation *per se*; at the same time, it is likely that mechanical ventilation is an additional contributor to the ^{18}FDG signal, because it can amplify the inflammatory stimulus. Another finding is that, when analyzing the regional distribution of K_i and specifically its relationship to lung density, two patterns could be found: in seven patients, ^{18}FDG uptake rate was highest in regions with the highest density and in three patients metabolic activity was higher in normally or poorly aerated regions than in nonaerated regions. In normal lungs, K_i is expected to increase linearly with lung density, as was indeed the case for our control subjects, because regions with higher lung density have relatively more parenchyma (and hence cells) and less air. The absence of such a correlation in three patients with ALI/ARDS could be explained by two factors. First, the less aerated tissue could have a lower metabolic activity than the more aerated tissue, but the effect of this difference on the K_i measurement would be offset or reduced by its lower air content, with an increased number of metabolically active cells in each voxel. Second, if the increase in lung density was caused by edema rather than by alveolar collapse, two regions with different densities as measured by CT could have similar cell mass per voxel and hence similar K_i. Further studies are required to investigate the causes underlying such different behaviors.

CONCLUSIONS

Despite the fact that these preliminary results need to be confirmed and expanded in a larger sample of patients, this study shows that in patients with ALI/ARDS, undergoing mechanical ventilation for days, the metabolic activity of the lung is substantially increased across the entire lung density spectrum. This suggests that no region of the lung is spared by the presence of activated inflammatory cells; the intensity of this activation and its regional distribution, however, vary widely within and between patients.

ACKNOWLEDGMENTS

We are indebted to the physicians, the nurses, and the technicians of the Intensive Care Unit and of the Department of Nuclear Medicine of San Gerardo Hospital, Monza, Italy. We thank Alberto Lucchini, RN, Claudia Pasquali, BS, Elena DePonti, BS, and Antonio Perri, Radiation Technician for their technical assistance. We thank Jose G. Venegas, PhD, (Department of Anesthesia and Critical Care, Massachusetts General Hospital, Harvard Medical School, Boston, MA) for his useful comments and insights; John J. Marini, MD, (Pulmonary and Critical Care Medicine, University of Minnesota, St. Paul, MN) for critical revision of the manuscript; and Luciano Gattinoni, MD, FRCP, (Istituto di Anestesiologia e Rianimazione, Università degli Studi di Milano, Milan, Italy) for his help and suggestions.

REFERENCES

1. Wheeler AP, Bernard GR: Acute lung injury and the acute respiratory distress syndrome: A clinical review. *Lancet* 2007; 369: 1553–1564
2. Rubenfeld GD, Caldwell E, Peabody E, et al: Incidence and outcomes of acute lung injury. *N Engl J Med* 2005; 353:1685–1693
3. Yilmaz M, Iscimen R, Keegan MT, et al: Six-month survival of patients with acute lung injury: Prospective cohort study. *Crit Care Med* 2007; 35:2303–2307
4. Gattinoni L, Pesenti A: The concept of "baby lung." *Intensive Care Med* 2005; 31:776–784
5. Lee WL, Downey GP: Neutrophil activation and acute lung injury. *Curr Opin Crit Care* 2001; 7:1–7
6. Abraham E: Neutrophils and acute lung injury. *Crit Care Med* 2003; 31(Suppl 4):S195–S199
7. Wittkowski H, Sturrock A, van Zoelen MA, et al: Neutrophil-derived S100A12 in acute lung

injury and respiratory distress syndrome. *Crit Care Med* 2007; 35:1369–1375
8. Laufe MD, Simon RH, Flint A, et al: Adult respiratory distress syndrome in neutropenic patients. *Am J Med* 1986; 80:1022–1026
9. Sugiura M, McCulloch PR, Wren S, et al: Ventilator pattern influences neutrophil influx and activation in atelectasis-prone rabbit lung. *J Appl Physiol* 1994; 77:1355–1365
10. Kawano T, Mori S, Cybulsky M, et al: Effect of granulocyte depletion in a ventilated surfactant-depleted lung. *J Appl Physiol* 1987; 62: 27–33
11. Karzai W, Cui X, Heinicke N, et al: Neutrophil stimulation with granulocyte colony-stimulating factor worsens ventilator-induced lung injury and mortality in rats. *Anesthesiology* 2005; 103:996–1005
12. Jones HA: Inflammation imaging. *Proc Am Thorac Soc* 2005; 2:545–548, 513–544
13. Schuster DP: The evaluation of lung function with PET. *Semin Nucl Med* 1998; 28:341–351
14. Musch G, Venegas JG: Positron emission tomography imaging of regional lung function. *Minerva Anestesiol* 2006; 72:363–367
15. Schroeder T, Vidal Melo MF, Musch G, et al: PET imaging of regional 18F-FDG uptake and lung function after cigarette smoke inhalation. *J Nucl Med* 2007; 48:413–419
16. Taylor IK, Hill AA, Hayes M, et al: Imaging allergen-invoked airway inflammation in atopic asthma with [18F]-fluorodeoxyglucose and positron emission tomography. *Lancet* 1996; 347:937–940
17. Chen DL, Rosenbluth DB, Mintun MA, et al: FDG-PET imaging of pulmonary inflammation in healthy volunteers after airway instillation of endotoxin. *J Appl Physiol* 2006; 100: 1602–1609
18. Jones HA, Sriskandan S, Peters AM, et al: Dissociation of neutrophil emigration and metabolic activity in lobar pneumonia and bronchiectasis. *Eur Respir J* 1997; 10:795–803
19. Jones HA, Clark RJ, Rhodes CG, et al: In vivo measurement of neutrophil activity in experimental lung inflammation. *Am J Respir Crit Care Med* 1994; 149:1635–1639
20. Musch G, Venegas JG, Bellani G, et al: Regional gas exchange and cellular metabolic activity in ventilator-induced lung injury. *Anesthesiology* 2007; 106:723–735
21. Hartwig W, Carter EA, Jimenez RE, et al: Neutrophil metabolic activity but not neutrophil sequestration reflects the development of pancreatitis-associated lung injury. *Crit Care Med* 2002; 30:2075–2082
22. Chen DL, Schuster DP: Positron emission tomography with [18F]fluorodeoxyglucose to evaluate neutrophil kinetics during acute lung injury. *Am J Physiol Lung Cell Mol Physiol* 2004; 286:L834–L840
23. Jones HA, Schofield JB, Krausz T, et al: Pulmonary fibrosis correlates with duration of tissue neutrophil activation. *Am J Respir Crit Care Med* 1998; 158:620–628
24. Sandiford P, Province MA, Schuster DP: Distribution of regional density and vascular permeability in the adult respiratory distress syndrome. *Am J Respir Crit Care Med* 1995; 151(3 Pt 1):737–742
25. Maunder RJ, Shuman WP, McHugh JW, et al: Preservation of normal lung regions in the adult respiratory distress syndrome. Analysis by computed tomography. *JAMA* 1986; 255: 2463–2465
26. Perkins GD, Chatterjie S, McAuley DF, et al: Role of nonbronchoscopic lavage for investigating alveolar inflammation and permeability in acute respiratory distress syndrome. *Crit Care Med* 2006; 34:57–64
27. Papazian L, Doddoli C, Chetaille B, et al: A contributive result of open-lung biopsy improves survival in acute respiratory distress syndrome patients. *Crit Care Med* 2007; 35: 755–762
28. Bernard GR, Artigas A, Brigham KL, et al: The American-European Consensus Conference on ARDS. Definitions, mechanisms, relevant outcomes, and clinical trial coordination. *Am J Respir Crit Care Med* 1994; 149(3 Pt 1): 818–824
29. Warner MA, Divertie MB, Offord KP, et al: Clinical implications of variation in total venoarterial shunt fraction calculated by different methods during severe acute respiratory failure. *Mayo Clin Proc* 1983; 58: 654–659
30. Schiepers C, Nuyts J, Wu HM, et al: PET with 18F-fluoride: Effects of interactive versus filtered backprojection reconstruction on kinetic modeling. *IEEE Trans Nucl Sci* 1997; 44:1591–1593
31. Lubberink M, Boellaard R, van der Weerdt AP, et al: Quantitative comparison of analytic and iterative reconstruction methods in 2- and 3-dimensional dynamic cardiac 18F-FDG PET. *J Nucl Med* 2004; 45:2008–2015
32. Sondergaard HM, Madsen MM, Boisen K, et al: Evaluation of iterative reconstruction (OSEM) versus filtered back-projection for the assessment of myocardial glucose uptake and myocardial perfusion using dynamic PET. *Eur J Nucl Med Mol Imaging* 2007; 34:320–329
33. Patlak CS, Blasberg RG, Fenstermacher JD: Graphical evaluation of blood-to-brain transfer constants from multiple-time uptake data. *J Cereb Blood Flow Metab* 1983; 3:1–7
34. De Geus-Oei LF, Visser EP, Krabbe PF, et al: Comparison of image-derived and arterial input functions for estimating the rate of glucose metabolism in therapy-monitoring 18F-FDG PET studies. *J Nucl Med* 2006; 47:945–949
35. Oehler R, Weingartmann G, Manhart N, et al: Polytrauma induces increased expression of pyruvate kinase in neutrophils. *Blood* 2000; 95:1086–1092
36. Musch G, Layfield JD, Harris RS, et al: Topographical distribution of pulmonary perfusion and ventilation, assessed by PET in supine and prone humans. *J Appl Physiol* 2002; 93:1841–1851
37. Musch G, Bellani G, Vidal Melo MF, et al: Relation between shunt, aeration and perfusion in experimental acute lung injury *Am J Respir Crit Care Med* 2008; 177:292–300
38. Stewart EE, Chen X, Hadway J, et al: Correlation between hepatic tumor blood flow and glucose utilization in a rabbit liver tumor model. *Radiology* 2006; 239:740–750
39. Dunn RT, Willis MW, Benson BE, et al: Preliminary findings of uncoupling of flow and metabolism in unipolar compared with bipolar affective illness and normal controls. *Psychiatry Res* 2005; 140:181–198
40. Ronnemaa EM, Ronnemaa T, Utriainen T, et al: Decreased blood flow but unaltered insulin sensitivity of glucose uptake in skeletal muscle of chronic smokers. *Metabolism* 1999; 48:239–244
41. Nuutila P, Raitakari M, Laine H, et al: Role of blood flow in regulating insulin-stimulated glucose uptake in humans. Studies using bradykinin, [15O]water, and [18F]fluorodeoxy-glucose and positron emission tomography. *J Clin Invest* 1996; 97:1741–1747
42. Pitkanen OP, Laine H, Kemppainen J, et al: Sodium nitroprusside increases human skeletal muscle blood flow, but does not change flow distribution or glucose uptake. *J Physiol* 1999; 521 (Pt 3):729–737
43. Paquet N, Albert A, Foidart J, et al: Within-patient variability of (18)F-FDG: Standardized uptake values in normal tissues. *J Nucl Med* 2004; 45:784–788
44. Hadi M, Bacharach SL, Whatley M, et al: Glucose and insulin variations in patients during the time course of a FDG-PET study and implications for the "glucose-corrected" SUV. *Nucl Med Biol* 2008; 35:441–445
45. Kaplan JD, Calandrino FS, Schuster DP: A positron emission tomographic comparison of pulmonary vascular permeability during the adult respiratory distress syndrome and pneumonia. *Am Rev Respir Dis* 1991; 143: 150–154
46. Zhang H, Downey GP, Suter PM, et al: Conventional mechanical ventilation is associated with bronchoalveolar lavage-induced activation of polymorphonuclear leukocytes: A possible mechanism to explain the systemic consequences of ventilator-induced lung injury in patients with ARDS. *Anesthesiology* 2002; 97:1426–1433
47. Choudhury S, Wilson MR, Goddard ME, et al: Mechanisms of early pulmonary neutrophil sequestration in ventilator-induced lung injury in mice. *Am J Physiol Lung Cell Mol Physiol* 2004; 287:L902–L910
48. Muscedere JG, Mullen JB, Gan K, et al: Tidal ventilation at low airway pressures can augment lung injury. *Am J Respir Crit Care Med* 1994; 149:1327–1334
49. Caironi P, Ichinose F, Liu R, et al: 5-Lipoxygenase deficiency prevents respiratory failure during ventilator-induced lung injury. *Am J Respir Crit Care Med* 2005; 172:334–343